Received: 12 February 2022 | Revised: 16 July 2022 | Accepted: 18 July 2022

DOI: 10.1049/mia2.12285

IET Microwaves, Antennas & Propagation

ORIGINAL RESEARCH

Evaluation of admittance domain behavioural model complexity requirements for Power Amplifier design

Maria Rocio Moure[1] | **Michael Casbon[2]** | **Nicolas Ladero[1]** | **Monica Fernandez-Barciela[1]** | **Paul J. Tasker[2]**

[1]atlanTTic Research Center, Universidade de Vigo, Vigo, Spain

[2]Cardiff School of Engineering, Cardiff University, Cardiff, UK

Correspondence

Monica Fernandez-Barciela, atlanTTic Research Center, Universidade de Vigo C/ Maxwell s/n, 36310 Vigo, Spain.
Email: monica.barciela@uvigo.es

Funding information

Ministerio de Ciencia e Innovación (MCIN)/Agencia Estatal de Investigación (AEI)/10.13039/501100011033 and ERDF A way of making Europe, Grant/Award Number: TEC2017-88242-C3-2-R

Abstract

In the framework of Power Amplifier (PA) design for communications, frequency domain non-linear behavioural models have shown their potential as efficient complementary modelling tools when Field Effect Transistor compact models are not available or sufficiently accurate. The Admittance behavioural model, formulated in the V-I domain, is especially suitable for device size and fundamental frequency scaling. It is important to note that the direct extraction of this model, from the Nonlinear Vector Network Analyser (NVNA) load-pull (LP) measurements, requires some extra processing since it necessitates a Look-up-Table indexed to $|V_{11}|$ rather than $|A_{11}|$. When using such models in PA design, there is the need for the user to select the necessary model complexity. To address this requirement, in this paper, a systematic analysis methodology, to guide the user, is presented and validated in different PA design scenarios. The methodology was tested using NVNA LP measurements of GaN Heterostructure FETs. A fifth order Admittance model formulation showed good accuracy in the studied PA design scenarios.

1 | INTRODUCTION

The practical implementation of new communication systems, in which carrier signals are moved to less populated bands of the electromagnetic spectrum, allowing for higher bandwidth and increased data rates, coupled with adequate RF power levels, high energy efficiency and bandwidth efficient modulation schemes, impose critical demands on the RF transceiver design. One of the key elements in this module is the RF Power Amplifier (PA) on the transmitter part, which design demands state-of-the-art transistor technologies and circuit architectures; hence, the significance of accurate non-linear (NL) simulation and modelling tools. The use of new transistor technologies, capable of high power at high frequencies, or multi-transistor PA architectures often limits the availability or accuracy of NL compact/analytical Field Effect Transistor (FET) models needed in Computer Aided Design (CAD) due to the long time required for extensive active device characterisation, model extraction and validation to be undertaken. In this context, frequency domain behavioural models can provide a useful alternative solution.

The most popular frequency domain behavioural approach is the s-parameter model, which describes time-invariant linear device behaviour (in the steady-state) in terms of complex-valued linear algebraic maps of normalized voltage incident and scattered travelling waves (A-B domain). This model is fully consistent with VNA-based measurement systems since they measure the complex ratio of B to A wave phasors.

There have been different approaches to extend s-parameters to NL operation, among them are the Polyharmonic Distortion (PHD) [1] and Cardiff [2] behavioural models. Both also rely on the time-invariant assumption, besides using complex-valued NL algebraic maps of A-B waves and commensurate frequency components. While PHD model formulation can be simplified through linearization of the NL describing functions for the small power spectral components (harmonic superposition) around a large-signal operating point (LSOP), to provide a manageable set of NL parameters (X-parameters), the Cardiff model does not impose such restriction. Both models are formulated in terms of harmonic stimuli A_{ph} phase-normalized to the fundamental large-signal input stimulus A_{11}, thus requiring an un-normalizing procedure to restore the phase of the output spectral components.

In unmatched environments, X-parameters predictions can be improved by expanding the Look-up-Table (LUT) indexing to also include the load-pull (LP) reflection coefficients [3]. The Cardiff approach is conceptually well suited for highly unmatched terminations, or when PA design involve harmonic LP on extensive areas on the Smith Chart and/or high compression levels, as in the case of high efficiency PA design. In the Cardiff model, simply by increasing the order of the NL spectral interactions, hence the number of behavioural parameters, it is possible to achieve high model accuracy with a LUT not indexed to the LP reflection coefficients.

The challenge for the model user is to define, hence know in advance, which order of non-linearity suits the application. If the order chosen is too low, the model will not be accurate enough; if it is too high, then excessively large datasets will have been measured to extract the model parameters needlessly and simulations times will be unnecessarily slower, in the best of cases, or even unstable. To provide some guidance on the Cardiff model order best suited for a given PA design, the authors have developed and presented a systematic approach to determine the best NL order and parameters to predict performance, addressing the 1dB to 3dB gain compression impedance design space, required for the case of load-pulling the fundamental load impedance only; harmonic impedances were set to 50 Ω [4].

Note these models are formulated in the A-B domain. However, for modelling transistors, the Admittance V-I domain would be more physical. In recent years, several alternative admittance behavioural formulations have been proposed [5–9]. They basically follow the same assumptions behind X-parameters or the Cardiff model and require phase normalization, but their formulations consist of NL algebraic maps of (total) voltages and currents phasors, for the different spectral components, at the transistor ports (V-I domain). The advantages for utilizing Admittance model V-I formulation in CAD, over the previous A-B approaches, is their suitability for transistor size scaling and fundamental frequency (f_0) scaling [6–9]. For example, in Ref. [6], both FET size and frequency linear scaling were proved, in Ref. [9], frequency linear scaling, while in Ref. [8], a more complex (quadratic) frequency scaling was tested.

One drawback of the Admittance V-I LUT Cardiff model solution is that it is more difficult to be extracted than the original A-B LUT Cardiff model, since Admittance LUT behavioural models requires indexing to the fundamental large-signal input voltage $|V_{11}|$ (and phase normalized with respect to it too) instead of indexing to $|A_{11}|$. Non-linear Vector Network Analyser (NVNA) systems do not have voltage sources, but power sources, so fix the value of $|A_{11}|$ but not $|V_{11}|$. Hence, to extract a V-I domain-based LUT model, rather than an A-B domain-based LUT model, there is a need to translate $|A_{11}|$ indexed LP measured datasets to a $|V_{11}|$ indexed datasets, as part of the admittance model parameter extraction process. An approach has been developed by the authors to allow for the direct extraction of V-I admittance LUT models index to $|V_{11}|$ from conventional LP measurements [10]. The additional complexity required for extracting the Admittance model is probably one of the reasons behind the lack of more publications on this topic, to date.

As in the case of the A-B Cardiff model formulation, in the V-I Admittance Cardiff model formulation, there is still a requirement for the user to define which order of non-linearity is best suited to the application, to avoid inaccurate results, simulation instabilities or time-consuming transistor characterizations and slow simulation times. In this paper, a systematic investigation is performed to determine the required Admittance model complexity to provide an efficient tool in waveform engineered PA design. This paper extends a preliminary work in Ref. [11], in which a general and limited study was performed with admittance models extracted from simulations and measurements but using fundamental only LP, at two different gain compression levels. In this work an extended complexity analysis is undertaken, fully focussed on determining the best model formulations for accurate PA design. The approach developed will be first verified using simulated data and then applied to NVNA measurements. Two different GaN Heterostructure FET (HFET) technologies are considered, going beyond [11] by probing different device sizes, bias points, fundamental frequencies, compression levels and multi-harmonic injections.

In Section 2, a brief description of the Admittance behavioural model used is provided. In Section 3, some conclusions from the preliminary complexity analysis in Ref. [11] are summarized and an error metric defined. In Section 4, different complexity Admittance models are extracted using "measurements" obtained through simulations of a foundry model and are systematically evaluated in diverse extraction and PA design scenarios, all in the framework of Class B/J PA design. Finally, in Section 5, these models are extracted from f_0 and $2f_0$ NVNA LP measurements at higher levels of compression, and evaluations of the best model candidates are shown. Some guidance is given to the PA designer through the summary in the conclusions section of this work.

2 | ADMITTANCE BEHAVIOURAL MODEL FORMULATION AND EXTRACTION

The Admittance behavioural model described in this paper follows, as the Cardiff model, the theory of mixing in a non-linear device, and both share similar assumptions and related formulations. The Admittance model is formulated in the complex V-I phasor domain, where $I_{p,h}$ are the response complex amplitudes to the applied $V_{p,h}$ complex amplitudes of the excitations and are described by polynomial expansion in magnitude and relative phase. We assume commensurate frequency components and phase normalisation to $\angle V_{11}$.

The model mathematical formulation is shown in (1), characterising the NL interactions between the spectral components in the system and providing the steady-state response of the system linked to the LSOP. The NL behavioural coefficients $N_{p,h,i}$ are then function of the fundamental frequency, the magnitude of the driving input voltages $|V_{11}|$, hence the need for a $N_{p,h.i}$ parameter LUT indexed to $|V_{11}|$, and the active device bias point.

$$I_{p,h} = \sum_{i=0}^{W} N_{p,h.i}\left(\left|V_{1,1}\right|\right)\left|V_{2,1}\right|^{a_i} Q_{2,1}^{b_i} \cdots \left|V_{q,n}\right|^{y_i} Q_{q,n}^{z_i} \quad (1)$$

In (1), 'Q_n' is the phase term for V_{2n}, $e^{jn<V_{2n}}$,'p' and 'q' are the port indices, and 'h' and 'n' are the harmonic indices. 'W' is the total number of terms in the non-linear describing function. Note, from the theory of mixing the index parameters within the pairs $\{a_i, b_i\}$ and $\{y_i, z_i\}$ are related, for example, in the term$\left|V_{2,1}\right|^{a_i} Q_{2,1}^{b_i}$, the magnitude index ($a_i$) is related with the phase index (b_i) as follows:

$$a_i = |b_i| + 2r_i \quad (2)$$

where 'r_i' are positive stepped integer quantities, 0, 1, 2…

In this paper, the Admittance model complexity is truncated by either the maximum allowed mixing order and/or the maximum values defined for the model indices, that is, $|b|$ and r.

If, for simplification purposes, the second harmonic ($2f_0$) load is set to a short circuit and then V_{22} is zero; so only V_{21} is included in the formulation, as shown in (3).

$$I_{p,h} = \sum_{i=0}^{W} N_{p,h.i}\left(\left|V_{1,1}\right|\right)\left|V_{2,1}\right|^{a_i} Q_{2,1}^{b_i} \quad (3)$$

Table 1 shows possible combinations of $|V_{21}|$ and Q_{21} powers in (3), with their corresponding lowest mixing order identified, for dc, f_0 and $2f_0$ predictions. Table 2 shows examples of the resulting $I_{p,1}$ NL describing function obtained for increasing $|b|$ and r indices, if third order mixing is the maximum allowed.

In this paper, different scenarios were analysed to determine the most suitable model complexity for a given application. In general, model formulation used is defined up to second harmonic terms, and without assuming $V_{2,2}$ always zero, as in (4).

$$I_{p,h} = \sum_{i=0}^{W} N_{p,h.i}\left(\left|V_{1,1}\right|\right)\left|V_{2,1}\right|^{a_i} Q_{2,1}^{b_i}\left|V_{2,2}\right|^{c_i} Q_{2,2}^{d_i} \quad (4)$$

Note,

$$c_i = |d_i| + 2s_i \quad (5)$$

where s_i are positive stepped integer quantities, 0, 1, 2…

In the case of the model extraction from NVNA measurements, $|A_{11}|$ indexed data has been used with the intermediate formulation for the Admittance model defined in Ref. [10]. That formulation is compatible with measurements at a fixed $|A_{11}|$ but includes the variations of $|V_{11}|$ due to LP. This procedure causes a temporary increase in the number of behavioural coefficients because of the additional terms used to account for V_{11} varying. These intermediate coefficients are then used to determine the LUT coefficients $N_{p,h,i}$ indexed to the average $|V_{11}|$, hence generating the model defined in (4).

3 | COMPLEXITY ANALYSIS AND ERROR FIGURE OF MERIT

The methodology used in this paper for the complexity analysis consists of generating different models, by varying in (4) the NL order and maximum indices, values $|b|$ and r, then analysing the resulting number of behavioural parameters and the quality of the model predictions for dc, f_0 and second harmonic, for different LP conditions. To aid in determining the model prediction quality, we defined an error figure of merit (FOM), shown in (6), in which the sum is the over all LP impedances involved:

$$\mathrm{FOM} = 20\log_{10}\left(\sqrt{\frac{\sum\left(\left|I - I_{\mathrm{model}}\right|^2\right)}{\sum\left(\left|I\right|^2\right)}}\right)\ (\mathrm{dBc}) \quad (6)$$

Note that $I_{p,1}$ and $I_{p,2}$ FOM's informs about the model's capability for waveform engineering in PA design. The DC FOM informs about the accuracy on the efficiency prediction.

From the preliminary steps undertaken in Ref. [11], we soon drew some basic conclusions:

(1) When maximum $|b|$ is limited to 0, model results are poor.

The small-signal admittance model (linear y-parameters) is defined by the following coefficients: $|b| = 0$, $r = 0$ (y_{21}) and $|b| = 1$, $r = 0$ (y_{22}); hence maximum value for index $|b|$ needs to be at least equal to 1 for a non-linear formulation.

(2) All formulations are limited to maximum $r = 1$.

To avoid possible problems of overfitting in magnitude, if we let r index raise up to 2, it requires adding the next magnitude power term $\left|V_{2,1}\right|^{|b|+4}$.

Besides, we stablished −30 dBc FOM value as a reasonably good model prediction, which corresponds to a 3% of mean error. On occasion, −40 dBc could be used (1% error), but this value is difficult to achieve in practice, when using NVNA measurements, due to the measurement errors and noise fluctuations.

4 | MODEL COMPLEXITY ANALYSIS WITH SIMULATIONS

For the analysis in this section, we have used the WIN Semiconductors foundry model of a 4 × 125 μm GaN HFET. "Measurement data" was obtained from simulations with this model, performed with an input power source with

TABLE 1 Terms in (3) based on phase and magnitude indices values

DC		b: −2	−1	0	1	2
r	0	$\lvert V_{21}\rvert^2 Q^{-2}$ (4th order)	$\lvert V_{21}\rvert^1 Q^{-1}$ (2nd order)	$\lvert V_{21}\rvert^0 Q^0$ (order 0)	$\lvert V_{21}\rvert^1 Q^1$ (2nd order)	$\lvert V_{21}\rvert^2 Q^2$ (4th order)
	1	$\lvert V_{21}\rvert^4 Q^{-2}$ (6th order)	$\lvert V_{21}\rvert^3 Q^{-1}$ (4th order)	$\lvert V_{21}\rvert^2 Q^0$ (2nd order)	$\lvert V_{21}\rvert^3 Q^1$ (4th order)	$\lvert V_{21}\rvert^4 Q^2$ (6th order)
f_0		**b: −2**	**−1**	**0**	**1**	**2**
r	0	$\lvert V_{21}\rvert^2 Q^{-2}$ (5th order)	$\lvert V_{21}\rvert^1 Q^{-1}$ (3rd order)	$\lvert V_{21}\rvert^0 Q^0$ (1st order)	$\lvert V_{21}\rvert^1 Q^1$ (1st order)	$\lvert V_{21}\rvert^2 Q^2$ (3rd order)
	1	$\lvert V_{21}\rvert^4 Q^{-2}$ (7th order)	$\lvert V_{21}\rvert^3 Q^{-1}$ (5th order)	$\lvert V_{21}\rvert^2 Q^0$ (3rd order)	$\lvert V_{21}\rvert^3 Q^1$ (3rd order)	$\lvert V_{21}\rvert^4 Q^2$ (5th order)
$2f_0$		**b: −2**	**−1**	**0**	**1**	**2**
r	0	$\lvert V_{21}\rvert^2 Q^{-2}$ (6th order)	$\lvert V_{21}\rvert^1 Q^{-1}$ (4th order)	$\lvert V_{21}\rvert^0 Q^0$ (2nd order)	$\lvert V_{21}\rvert^1 Q^1$ (2nd order)	$\lvert V_{21}\rvert^2 Q^2$ (2nd order)
	1	$\lvert V_{21}\rvert^4 Q^{-2}$ (8th order)	$\lvert V_{21}\rvert^3 Q^{-1}$ (6th order)	$\lvert V_{21}\rvert^2 Q^0$ (4th order)	$\lvert V_{21}\rvert^3 Q^1$ (4th order)	$\lvert V_{21}\rvert^4 Q^2$ (4th order)

TABLE 2 Admittance model formulation limited to third order mixing

Max b	Max r	Formulation
0	0	$I_{p,b} = N_{p,b,0}(\lvert V_{11}\rvert)$
1	0	$I_{p,b} = N_{p,b,0}(\lvert V_{11}\rvert) + N_{p,b,1}(\lvert V_{11}\rvert)V_{21} + N_{p,b,2}(\lvert V_{11}\rvert)V_{21}^*$
1	1	$I_{p,b} = N_{p,b,0}(\lvert V_{11}\rvert) + N_{p,b,1}(\lvert V_{11}\rvert)V_{21} + N_{p,b,2}(\lvert V_{11}\rvert)V_{21}^* + N_{p,b,3}(\lvert V_{11}\rvert)\lvert V_{21}\rvert^2 + N_{p,b,4}(\lvert V_{11}\rvert)V_{21}\lvert V_{21}\rvert^2$
2	0	$I_{p,b} = N_{p,b,0}(\lvert V_{11}\rvert) + N_{p,b,1}(\lvert V_{11}\rvert)V_{21} + N_{p,b,2}(\lvert V_{11}\rvert)V_{21}^* + N_{p,b,3}(\lvert V_{11}\rvert)V_{21}^2$

f_0 = 5.4 GHz, and at approximately the Class B bias point: $V_{gs0} = -2.9$ V ($I_{ds0} = 0.36$ mA) and $V_{ds0} = 28$ V. Fundamental LP was performed around the optimum load, Z_{opt}, for maximum output power and at 1 dB compression input power, P_{1dB}.

As stated before, the extracted Admittance models were LUT indexed with $\lvert V_{11}\rvert$. It is important to note that while within a simulator, these behavioural models could have been directly extracted using "measured datasets" from simulations using voltage sources, but to obtain "measured LP datasets" similar to that only possible during NVNA LP measurements, we performed these simulations using power sources and applied the extraction technique described in Ref. [10]. Note, "measured LP datasets" at multiple values of input power, P_{in}, are required for this approach. Three consecutive values, around P_{1dB}: 20.5, 21 and 21.5 dBm were used in this case.

A set of Admittance models were extracted by varying the maximum mixing order from the 2nd to 11th order, while truncating the maximum phase index $\lvert b\rvert$ from 0 to 3, and the maximum magnitude index r from 0 to 2. We will limit the discussion in this section to the more relevant cases.

4.1 | Fundamental LP: 1 dB compression contours

In this section, a first analysis of the Admittance model complexity is performed. We limited the fundamental LP around Z_{opt} up to 1 dB compression, usually a critical Smith Chart design region in PA design. Second harmonic load is set to short circuit (as in Class B or F PA design); hence model formulation used in this section is simplified to (3).

In Figure 1 we show the more relevant Admittance model indices combinations, selected to work with a manageable number of model coefficients and minimise the $I_{2,i}$ FOM for dc, f_0 and $2f_0$. From the curves shown in Figure 1, the Admittance model with max $\lvert b\rvert = 1$ and max $r = 0$, and mixing up to the third order, is the simplest one that achieves or is close to the −30 dBc FOM level for dc and f_0. When using max $\lvert b\rvert = 1$, max $r = 1$ and mixing order up to 5, the FOM values for dc and f_0 are improved to close to −40 dBc, but the FOM value for the $2f_0$ prediction is still around −20 dBc. Only by increasing the mixing order up to seventh is it possible to achieve an FOM value at $2f_0$ close to −30 dBc, but at the expense of increasing the number of model coefficients.

Clearly by raising max r up to 1, FOM is, as expected, generally reduced, but we must consider that the number of coefficients is significantly increased. Note that dc and $2f_0$ model terms, shown in Table 1, use higher mixing order coefficients than f_0 terms, for $\lvert b\rvert = 1$ and $\lvert b\rvert = 2$, which explains why model prediction for f_0 improves dramatically when using a third order model, but dc and $2f_0$ predictions demand at least a fifth order model.

4.2 | Case study: Class B-J Power Amplifier design

As a case study, we will analyse the predictions of the behavioural model in the Smith Chart region involved in Class B-J PA design using the same HFET and $f_0 = 5.4$ GHz, and "dataset" provided by the foundry model. Figure 2 shows the extrinsic and intrinsic harmonic output loads for Class B [Figure 2a] and Class J [Figure 2b], and the f_0 LP efficiency and power contours [Figure 2c] up to 3 dB compression, around Z_{opt} for Class B, which includes Z_{opt} for Class J. Extrinsic $2f_0$ Z_L varies from almost a short circuit (Class B) to approximately 100j Ω (Class J). From this dataset, we identified that the 3 dB compression area in the f_0 output power contours would be enough for the Class B-J PA design. The Smith Chart region needed to be covered though LP at $2f_0$ involves the complete Smith Chart area within the $|\Gamma| = 1$ circle.

4.2.1 | Complexity analysis using fundamental and second harmonic load-pull

As indicated, we consider that the Smith Chart region in Figure 2c, covered by the LP up to 3 dB compression, around the Z_{opt}, is relevant at f_0, and that we need to cover the full Smith Chart for $2f_0$. These are the areas used in this section for the complexity analysis, with the same input power levels as in previous sections: 20.5, 21 and 21.5 dBm.

The new methodology used in this section followed three steps. First, we analyse model complexity with only LP at f_0 and a short circuit for $2f_0$, covering up to 3 dB compression around Z_{opt} for maximum power. In this case, the obtained results were similar as in Section 4.1, requiring fifth or seventh order models to achieve FOM error of −30 dBc: max $r = 1$ improves the precision substantially, and max $|b| = 2$ makes $2f_0$ error prediction closer to the reference FOM level.

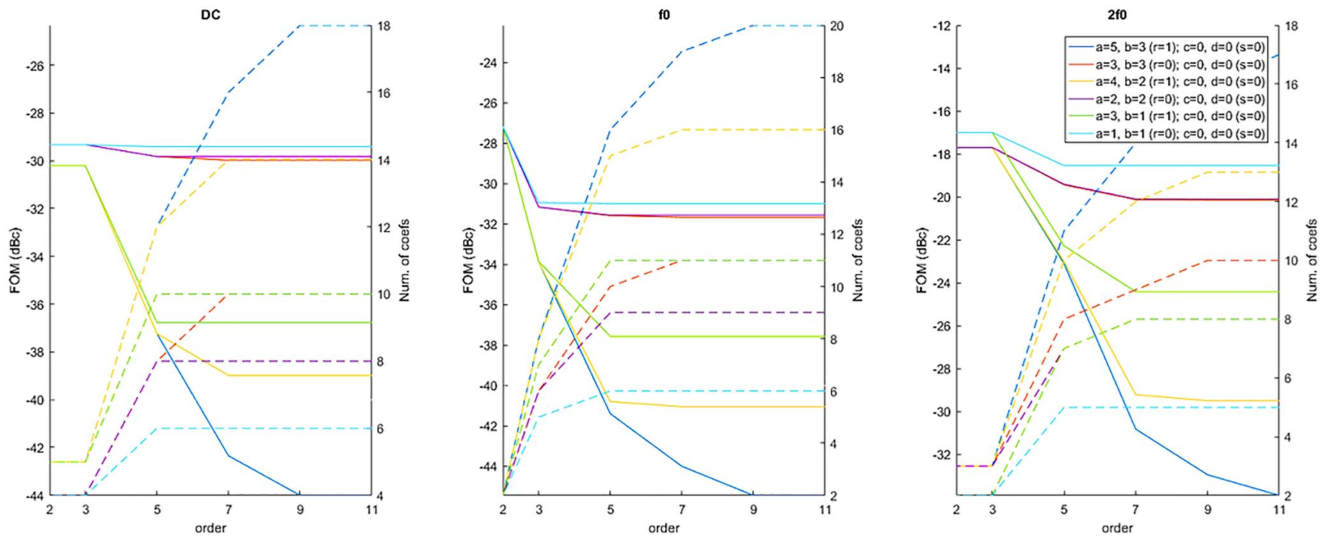

FIGURE 1 Accuracy in Admittance model predictions for dc, f_0 and $2f_0$, for different model complexities: figure of merit (FOM) (continuous lines), number of coefficients (dot line). 4 × 125 μm GaN HFET simulated fundamental Smith Charts design space within the 1dB load-pull (LP) power contour (WIN model). $f_0 = 5.4$ GHz. Mean V_{in}: 3.762 V

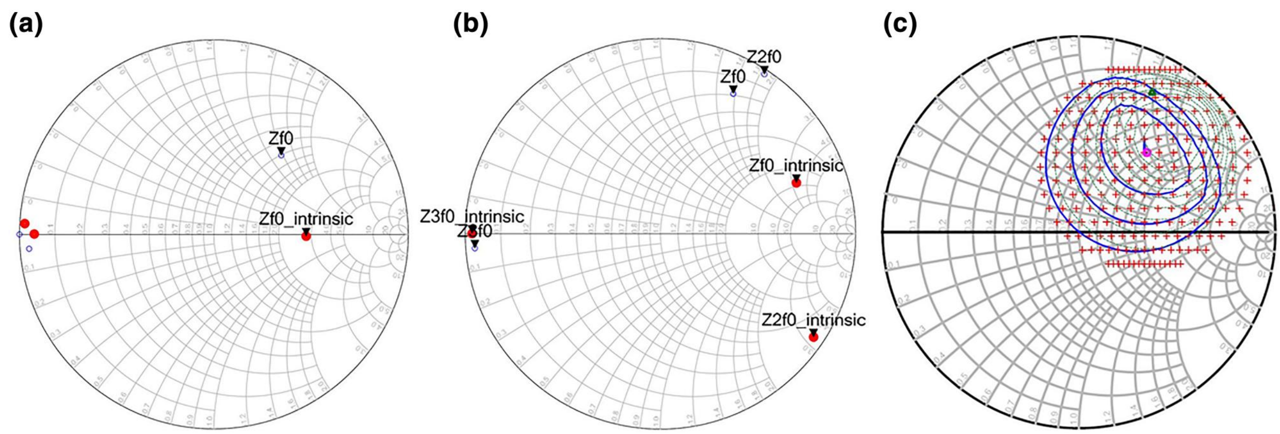

FIGURE 2 Smith Chart optimum extrinsic (blue circles) and intrinsic (red dots) load impedances for (a) Class B and (b) Class J. (c) Simulated (WIN model) f_0 load-pull (LP) efficiency (green striped lines) and power contours (blue solid lines) up to 3 dB compression, around Z_{opt} for max. Power at Class B (pink circle). Z_{opt} for max. Power for Class J is plotted too (green triangle), defining the Smith Chart design space. 4 × 125 μm GaN HFET. $f_0 = 5.4$ GHz. P_{in}: 21 dBm

Second, another study was performed with f_0 set to Z_{opt} and $2f_0$ load-pulling over the complete $|\Gamma| = 1$ circle. In this case, the Admittance model formulation in (4) was used. The results obtained revealed that increasing the maximum value for indices d and s did not significantly improve the model precision, from that, the best combination was max $|d| = 1$ and max $s = 0$. Third, a new study was performed, simultaneously load-pulling both f_0 and $2f_0$. Again, (4) was used. Figures 3 and 4 show the results of this third analysis, and they confirm that the previous ones are the more relevant for this case study.

Figure 3 shows how varying the maximum value for indices $|d|$ and s, with a fixed combination of maxima for indices $|b|$ and r, does not make a big impact on the prediction results. From this figure, it is apparent that the best model to use would be a combination of d and s that provides the smallest number of coefficients, that is max $|d| = 1$ and max $s = 0$.

Figure 4 and Table 3 show a group of selected combinations of $|b|$ and r with max $|d| = 1$ and max $s = 0$. It is noted, again, that max $r = 1$ greatly impacts the model precision. Since with third order models it is not possible to achieve the FOM reference level of -30 dBc, it would be necessary to at

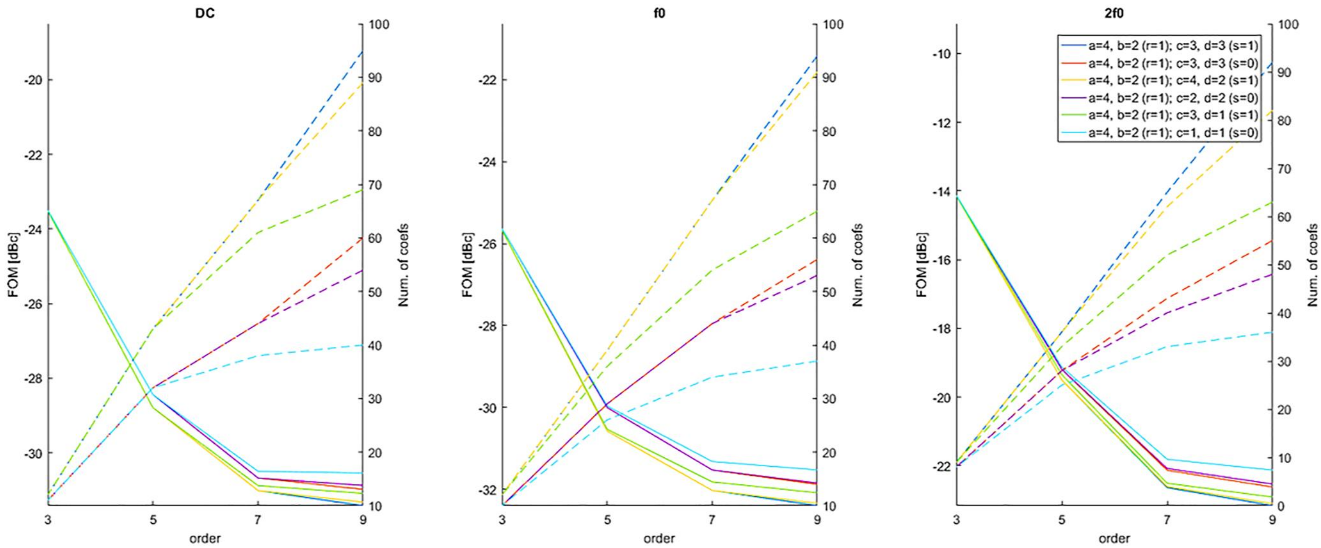

FIGURE 3 Accuracy in Admittance model predictions for dc, f_0 and $2f_0$ for different model complexities: figure of merit (FOM) (continuous lines) and number of coefficients (dot line). Example of different combinations of max d and max r with max $|b| = 2$ and max $r = 1$. 4 × 125 μm GaN HFET simulated Smith Chart design space within the 3 dB load-pull (LP) power contour for f_0 and over the whole Smith Chart for $2f_0$ (WIN model). $F_0 = 5.4$ GHz. Mean V_{in}: 3.897 V

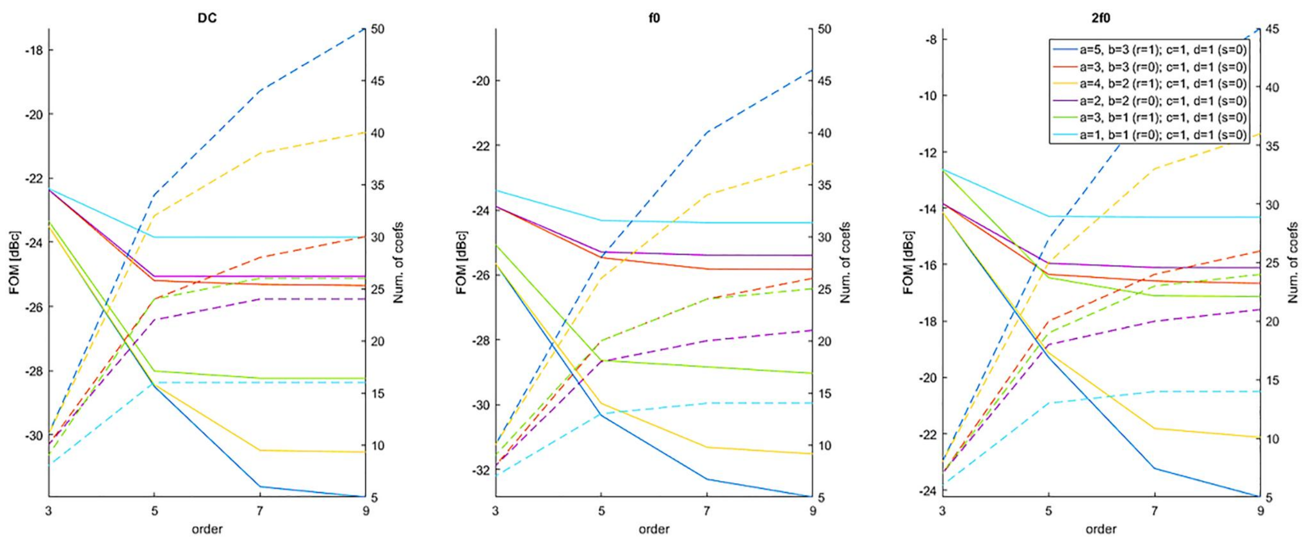

FIGURE 4 Accuracy in Admittance model predictions for dc, f_0 and $2f_0$ for different model complexities: figure of merit (FOM) (continuous lines) and number of coefficients (dot line). 4 × 125 μm GaN HFET simulated Smith Chart design space within the 3 dB load-pull (LP) power contour for f_0 and the whole Smith Chart for $2f_0$ (WIN model). $f_0 = 5.4$ GHz. Mean V_{in}: 3.897 V

least use the fifth mixing order. For max $|b| = 1$ and max $r = 1$ fifth order model, there is a noticeable improvement in the f_0 prediction, with FOM close to −30 dBc. Letting $|b|$ raise up to 2, does not improve the $2f_0$ prediction to below −20 dBc, unless mixing order is increased to the seventh order.

In Table 3, these observations are highlighted: in green, the model formulation showing acceptable performance with the least number of coefficients (fifth order model and maximum indices values of $|b| = 1, r = 1, |d| = 1$ and $s = 0$); and in blue, the one showing the best accuracy but still with a relatively low number of coefficients (seventh order model with max. Indices of $|b| = 2, r = 1, |d| = 1$ and $s = 0$). Note that results in Table 3 are ordered from the smaller FOM error at f_0 to the highest.

TABLE 3 Simulations: figure of merit (FOM) for fundamental and second harmonic load-pull (LP) (max $d = 1$, max $s = 0$)

Order	b	r	Coefs DC	Coefs f_0	Coefs $2f_0$	FOM DC	FOM f_0	FOM $2f_0$
7	3	1	44	40	39	-32	-32	-23
7	2	1	38	34	33	-30	-31	-22
5	3	1	34	28	27	-28	-30	-19
5	2	1	32	26	25	-28	-30	-19
7	1	1	26	24	23	-28	-29	-17
5	1	1	24	20	19	-28	-29	-16
7	3	0	28	24	24	-25	-26	-17
7	2	0	24	20	20	-25	-25	-16
5	3	0	24	20	20	-25	-25	-16
5	2	0	22	18	18	-25	-25	-16
7	1	0	16	14	14	-24	-24	-14
5	1	0	16	13	13	-24	-24	-14

5 | MODEL COMPLEXITY ANALYSIS FROM THE NON-LINEAR VECTOR NETWORK ANALYSER MEASUREMENTS

To test previous results in practical situations, Admittance behavioural models were extracted directly from NVNA f_0 and $2f_0$ LP measurements, following procedure in Section 4.2. Measurements were performed at Cardiff University's labs on a 4 × 50 μm GaN High Electron Mobility Transistor ($V_{gs0} = -2.45$ V, $V_{ds0} = 25$ V) from a different foundry and $f_0 = 8$ GHz.

The direct extraction method described in Ref. [10], was used to obtain $|V_{11}|$ indexed Admittance models. Hence, again LP measurements need to be performed at different drive levels. In this case, 3 values at consecutives P_{in}: 11, 12 and 13 dBm powers levels were used. The Smith Chart area of interest, and the measurements used, for f_0 covers up to 4 dB compression in some places, includes both optimal impedances for maximum power and max. Drain efficiency, and covers the full Smith Chart for $2f_0$.

As in Section 4.2, the maximum values of $|d|$ and s do not affect dramatically the performance of the extracted Admittance models. In this case, to reduce the total number of coefficients, we would recommend using max $|d| = 1$ and max $s = 0$.

Figure 5 shows the models performance by using max $|d| = 1$ and max $s = 0$. Again, max $r = 1$ improves the accuracy in the result substantially. DC FOM error is around or below −30 dBc for all the models considered in the figure. To reach this low FOM level for prediction at f_0, model order should be at least fifth, with max $r = 1$. Setting max $|b| = 1$ is sufficient for accurate f_0 prediction, but a max $|b| = 2$ improves the $2f_0$ prediction, providing the FOM error level close to −30 dBc.

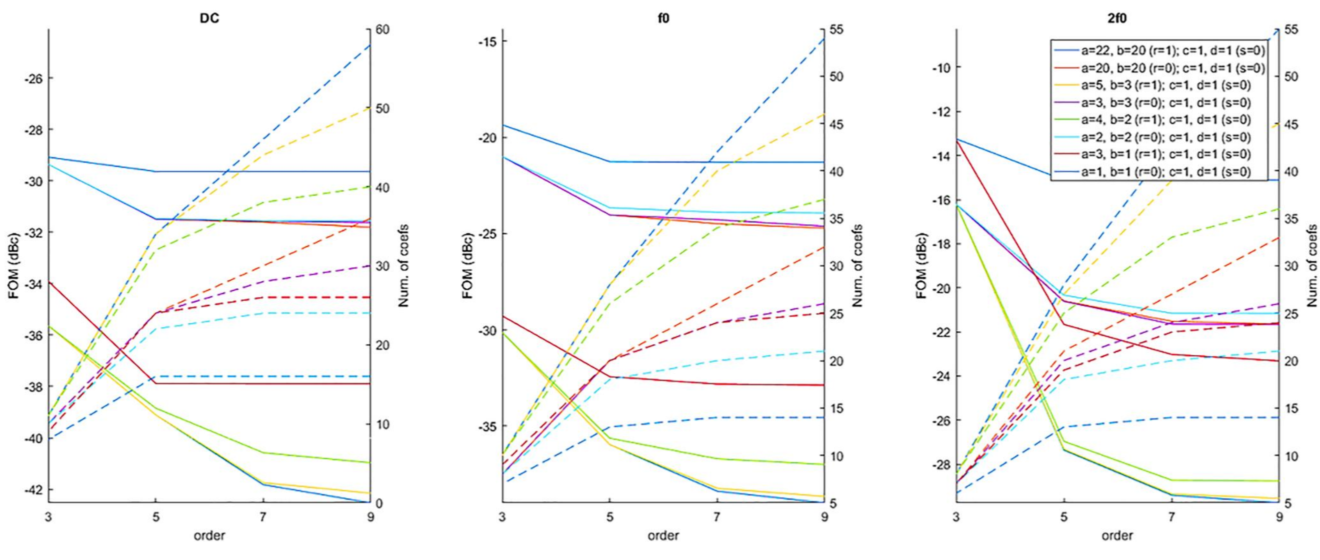

FIGURE 5 Accuracy in Admittance model predictions for dc, f_0 and $2f_0$ for different model complexities: figure of merit (FOM) (continuous lines) and number of coefficients (dot line). 4 × 50 μm GaN HFET Non-linear Vector Network Analyser (NVNA) meas. Smith Chart design space up to 4 dB load-pull (LP) power contour for f_0 and the whole Smith Chart for $2f_0$. $f_0 = 8$ GHz. Mean V_{in}: 1.796 V

TABLE 4 Measurements: figure of merit (FOM) for fundamental and second harmonic load-pull (LP) (max $d = 1$, max $s = 0$)

Order	b	r	Coefs DC	Coefs f_0	Coefs $2f_0$	FOM DC	FOM f_0	FOM $2f_0$
7	3	1	44	40	39	-42	-38	-29
7	2	1	38	34	33	-41	-37	-29
5	3	1	34	28	27	-39	-36	-27
5	2	1	32	26	25	-39	-36	-27
7	1	1	26	24	23	-38	-33	-23
5	1	1	24	20	19	-38	-32	-22
7	3	0	28	24	24	-32	-24	-22
7	2	0	24	20	20	-32	-24	-21
5	3	0	24	20	20	-31	-24	-21
5	2	0	22	18	18	-31	-24	-20
7	1	0	16	14	14	-30	-21	-15
5	1	0	16	13	13	-30	-21	-15

Table 4 shows the Admittance models precision and number of coefficients for fifth and seventh order in Figure 5. Marked in green is the Admittance model that, with the minimum number of coefficients, makes the FOM error in f_0 prediction lower than −30 dBc (fifth order model with maximum indices $|b| = 1$, $r = 1$, $|d| = 1$ and $s = 0$). With this model complexity, dc error FOM is close to −40 dBc, but for the $2f_0$ prediction it is still around −20 dBc. To improve the FOM in this case, a seventh order model with max $|b| = 2$ was required to get an error FOM for $2f_0$ prediction close to −30 dBc. Also improving dc and f_0 prediction too (around −40 dBc).

Figure 6 plots the power and efficiency contours for these two highlighted models in comparison with measurements. These results prove that both model formulations provide robust large-signal predictions, but some small differences can be appreciated: the seventh order model is slightly more accurate closer to the optimum impedance for power and efficiency.

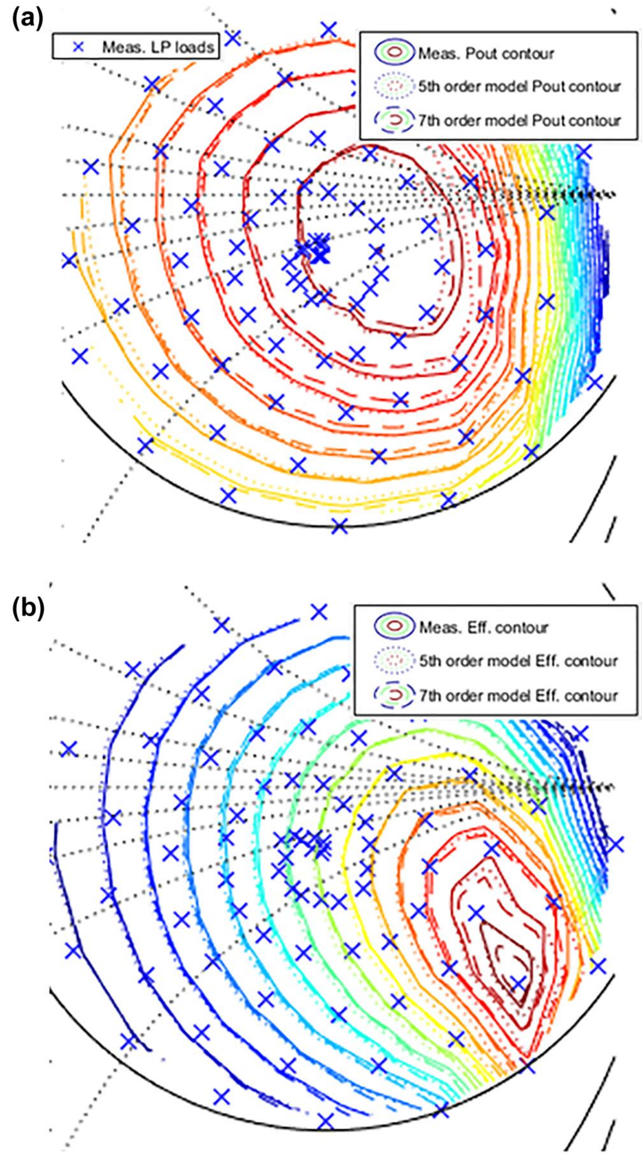

FIGURE 6 Admittance model predictions for power (a) and efficiency (b) contours versus the Non-linear Vector Network Analyser (NVNA) meas. 4 × 50 μm GaN HFET. Load-pull (LP) data up to 4 dB compression for f_0 and full $|\Gamma| \leq 1$ for $2f_0$. $f_0 = 8$ GHz. Mean V_{in}: 1.796 V

6 | CONCLUSION

The main goal for this study was to evaluate the optimum mixing order, and the associated set of secondary indices, to generate a precise Admittance model with the minimum number of NL coefficients, in the framework of waveform engineered PA design. A general conclusion after applying the proposed analysis methodology is that it is not necessary to use more than seventh order mixing complexity in the model. Variability on the maximum secondary indices and mixing order strongly depends on the application, always with the trade-off of higher precision and number of NL coefficients. More specific conclusions about the required model complexity for several PA design scenarios were achieved. For a quasi-linear design oriented to obtaining maximum output power, in which LP power contours up to 1 dB compression around the optimum load is the design critical area, a third order Admittance model, with maximum indices $|b| = 1$ and $r = 0$, provides adequate results. For higher precision, model complexity should be increased up to fifth order, with maximum $r = 1$. When the Smith Chart area of interest in the PA design is increased and more gain compressed transistor operation is required, for example, to also include the Z_{opt} for maximum efficiency, could require up to 3–4 dB gain compression, model complexity needs to be increased to include at least the fifth order terms, with maximum indices $|b| = 1$ and $r = 1$. A seventh order model with maximum $|b| = 2$ is the maximum necessary. For good precision on second harmonic LP, as required in Class B-J-F operation, maximum indices $|d| = 1$ and $s = 0$ provide good predictions.

ACKNOWLEDGEMENTS

The authors want to acknowledge WIN Semiconductors for providing device samples and corresponding NL model. This work was funded by the Ministerio de Ciencia e Innovación (MCIN)/Agencia Estatal de Investigación (AEI)/10.13039/501100011033 and by The European Regional Development Fund *A way of making Europe*, under grant TEC2017-88242-C3-2-R.

CONFLICT OF INTEREST

None of the co-authors have a conflict of interest to disclose

DATA AVAILABILITY STATEMENT

Data that support the findings of this study are not available and were used under licenses for the study.

ORCID

Maria Rocio Moure https://orcid.org/0000-0002-3910-9957

Monica Fernandez-Barciela https://orcid.org/0000-0002-3650-6068

REFERENCES

1. Verspecht, J., Root, D.E.: Polyharmonic distortion modeling. IEEE Microwave Mag. 7(3), 44–57 (2006). https://doi.org/10.1109/mmw.2006.1638289
2. Woodington, S., et al.: A novel measurement based method enabling rapid extraction of a RF waveform look-up table based behavioral model. IEEE MTT-S Int. Microwave Symp. Dig. 1453–1456 (2008)
3. Simpson, G., et al.: Load-pull + NVNA = Enhanced X-Parameters for PA Designs with High Mismatch and Technology-Independent Large-Signal Device Models. IEEE ARFTG Conf., Portland (2008)
4. Moure, M.R., et al.: A Systematic Investigation of Behavioural Model Complexity Requirements, pp. 77–80. EuMIC European Microw. Integrated Circuits Conf., Madrid (2018)
5. Fernandez-Barciela, M., et al.: Stretching the design: extending analytical circuit design from the linear to the nonlinear domain. IEEE Microwave Mag. 15(6), 106–120 (2014). https://doi.org/10.1109/mmm.2014.2332851
6. Koh, M., et al.: Frequency Scalable Large-Signal Transistor Behavioral Model Based on Admittance Domain Formulation. IEEE MTT-S Int. Microwave Symp., Tampa (2014)
7. Root, D.E., et al.: Frequency-scalable Nonlinear Behavioral Transistor Model from Single Frequency X-Parameters Based on Time-Reversal Transformation Properties. IEEE ARFTG Conf., USA (2015)
8. Moure, M.R., et al.: Broadband Non-linear FET Behavioral Model Defined in the Admittance Domain, pp. 281–284. EuMIC European Microw. Integrated Circuits Conf., London (2016)
9. Cai, J., et al.: A combined broadband model for GaN HEMTs in admittance domain based on canonical piecewise linear functions. IEEE Ttrans. on Microwave Theory and Tech. 68(12), 5042–5054 (2020). https://doi.org/10.1109/tmtt.2020.3021696
10. Moure, M.R., et al.: Direct Extraction of an Admittance Domain Behavioral Model from Large-Signal Load-Pull Measurements, pp. 1057–1060. IEEE MTT-S Int. Microw. Symp., Honolulu (2017)
11. Moure, M.R., et al.: A systematic investigation of admittance domain behavioral model complexity requirements. IEEE MTT-S Latin America Microw. Conf., Arequipa, Peru (2018)

How to cite this article: Moure, M.R., et al.: Evaluation of admittance domain behavioural model complexity requirements for Power Amplifier design. IET Microw. Antennas Propag. 1–9 (2022). https://doi.org/10.1049/mia2.12285